THE ASTROPHYSICAL JOURNAL, 550:L47–L51, 2001 March 20

THE PROMPT EMISSION OF GRB 990712 WITH *BEPPOSAX*: EVIDENCE OF A TRANSIENT X-RAY EMISSION FEATURE

F. FRONTERA,[1,2] L. AMATI,[2] M. VIETRI,[3] J. J. M. IN 'T ZAND,[4] E. COSTA,[5] M. FEROCI,[3] J. HEISE,[4] N. MASETTI,[2] L. NICASTRO,[6] M. ORLANDINI,[2] E. PALAZZI,[2] E. PIAN,[2] L. PIRO,[5] AND P. SOFFITTA[5]

Received 2000 October 4; accepted 2001 February 8; published 2001 March 15

ABSTRACT

We report on the prompt X- and γ-ray observations of GRB 990712 with the *BeppoSAX* Gamma-Ray Burst Monitor and Wide Field Camera 2. As a result of Sun constraints, we could not perform a follow-up observation with the *BeppoSAX* narrow-field instruments. The light curve of the prompt emission shows two pulses and a total duration of about 40 s in X-rays. In γ-rays, the event is even shorter. The 2–700 keV spectral emission with time shows a discontinuity in the peak energy E_p of the $EF(E)$ spectrum: E_p is above our energy passband during the first pulse and goes down to ~10 keV during the second pulse. Another peculiarity is noted in this event for the first time: the evidence of a 2 s duration emission feature during the tail of the first pulse. The feature is consistent with either a Gaussian profile with centroid energy of 4.5 keV or a blackbody spectrum with $kT_{bb} \sim 1.3$ keV. We discuss the possible origin of the feature. The most attractive possibility is that we are observing the thermal emission of a baryon-loaded expanding fireball when it becomes optically thin.

Subject headings: gamma rays: bursts — gamma rays: observations — shock waves — X-rays: general

1. INTRODUCTION

Observations of cosmic gamma-ray bursts (GRBs) with the *BeppoSAX* satellite are providing a key contribution to theories about their nature. Among the still unsettled questions, it is still not clear what are the mechanisms that produce the observed X-ray spectra and their evolution with time (see, e.g., Frontera et al. 2000) and what are the environments in which the GRBs occur. In the context of the internal shock model, synchrotron radiation is generally expected to play an important role in the production of the observed GRB spectra (e.g., Tavani 1996), but inverse Compton can also give a significant contribution to them (Ghisellini et al. 2000). Also, blackbody emission from the photosphere of the fireball (Mészáros & Rees 2000) is expected to contribute to the GRB spectra, and inhomogeneities in the GRB outflow, made of dense highly ionized metal-rich material, could give rise to broad spectral features, mainly K edges (Mészáros & Rees 1998). Effects of photoelectric absorption and Compton scattering from the circumburst material can modify the intrinsic energy spectrum of the GRBs, with the introduction of absorption cutoffs and features, such as K edges and emission lines (Mészáros & Rees 1998; Böttcher et al. 1999), the presence of which has already been reported for some GRBs (Yoshida et al. 1999; Piro et al. 1999, 2000; Antonelli et al. 2000; Amati et al. 2000). The separation of the intrinsic and external components is of key importance for establishing both the GRB emission mechanisms and the properties of the GRB environment.

The Gamma-Ray Burst Monitor (GRBM; 40–700 keV; Frontera et al. 1997) and the two Wide Field Cameras (WFCs; 2–28 keV; Jager et al. 1997) on board *BeppoSAX* offer the opportunity to study the GRB energy spectra in the 2–700 keV energy band, where the above components can be investigated (e.g., Frontera et al. 2000). GRB 990712 was detected by the WFC2 and the GRBM, showing in the 2–26 keV band the highest peak flux ever observed from a GRB with *BeppoSAX*. Its position was promptly distributed to the astronomical community (Frontera et al. 1999). Follow-up observations with the *BeppoSAX* narrow-field instruments were not possible because of Sun constraints. Observations were performed in the optical and radio bands. An optical transient with magnitude $R = 19.4 \pm 0.1$ was discovered about 3 hr after the event (Bakos et al. 1999), and its redshift is now well determined ($z = 0.4331 \pm 0.0004$; Vreeswijk et al. 2001).

2. OBSERVATIONS

GRB 990712 was detected on 1999 July 12, starting on 16:43:02 UT (Frontera et al. 1999). Its position was determined with an error radius of 2′ (99% confidence level) and was centered at $\alpha_{2000} = 22^h31^m50^s$, $\delta_{2000} = -73°24'24''$ (Heise et al. 1999). Features and data available from the GRBM and WFCs have already been reported in several papers (e.g., Frontera et al. 2000). The effective area exposed to the GRB was ≈420 cm^2 in the 40–700 keV band and 37 cm^2 in the 2–26 keV energy band. The background in the WFC and GRBM energy bands was fairly stable during the event. The WFC spectra were extracted through the iterative removal of sources procedure (e.g., Jager et al. 1997), which implicitly subtracts the contribution of the background and of other point sources in the field of view. The count rate spectra were analyzed using the XSPEC v.10 software package (Arnaud 1996). The quoted errors for the spectral parameters correspond to 90% confidence. Parameter values shown in brackets in Table 1 have been fixed while fitting.

3. RESULTS

Figure 1 shows the time profile of GRB 990712 in four energy bands after the background subtraction. In all bands the GRB shows a double-pulse structure, with an opposite behavior

[1] Dipartimento di Fisica, Università di Ferrara, Via Paradiso 12, 44100 Ferrara, Italy.
[2] Istituto Tecnologie e Studio Radiazioni Extraterrestri, CNR, Via Gobetti 101, 40129 Bologna, Italy.
[3] Dipartimento di Fisica, Terza Università di Roma, via della Vasca Navale, 84, 00146 Roma, Italy.
[4] Space Research Organization in the Netherlands, Sorbonnelaan 2, 3584 CA Utrecht, The Netherlands.
[5] Istituto Astrofisica Spaziale, CNR, Via Fosso del Cavaliere, 00133 Roma, Italy.
[6] Istituto Fisica Cosmica e Applicazioni all'Informatica, CNR, Via U. La Malfa 153, 90146 Palermo, Italy.

TABLE 1
SPECTRAL EVOLUTION OF GRB 990712 PROMPT EMISSION

Interval	Duration (s)	Model[a]	N_H[b]	α	β	E_p (keV)	χ^2/ν
A	4	Power law	3.2 ± 2.5	−1.40 ± 0.09	...	>700	7.8/6
	4	Power law	[0.0452]	−1.34 ± 0.07	...	...	10.0/7
B	2	Power law	2.7 ± 2.1	−1.44 ± 0.08	...	>700	4.4/5
	2	Power law	[0.0452]	−1.38 ± 0.06	...	...	7/6
C	2	Power law	0.3 ± 2.0	−1.66 ± 0.11	...	>700	16.0/6
	2	Power law	[0.0452]	−1.64 ± 0.07	...	...	16/7
D	4	Power law	[0.0452]	−1.80 ± 0.07	...	>700	4.6/6
E	2	Power law	[0.0452]	−2.04 ± 0.05	...	...	37/7
	2	Band law	[0.0452]	−0.4 ± 0.7	−2.4 ± 0.3	11 ± 8	3.5/5
F	3	Power law	[0.0452]	−2.01 ± 0.04	...	...	89/7
	3	Band law	[0.0452]	−0.7 ± 0.4	−2.3 ± 0.2	7 ± 3	4.3/5
G	7	Power law	[0.0452]	−2.15 ± 0.05	...	...	11/7
	7	Band law	[0.0452]	−1.6 ± 0.6	−2.3 ± 0.3	20 ± 15	2.5/5
H	7	Power law	[0.0452]	−2.3 ± 0.2	...	...	3.0/7

[a] The Band law refers to the smoothed broken power law proposed by Band et al. (1993); α and β are the power-law photon indices below and above the break energy E_0, respectively, and $E_p = E_0(2 + \alpha)$ is the peak energy of the $EF(E)$ spectrum.

[b] N_H-values are given in units of 10^{22} cm^{-2}.

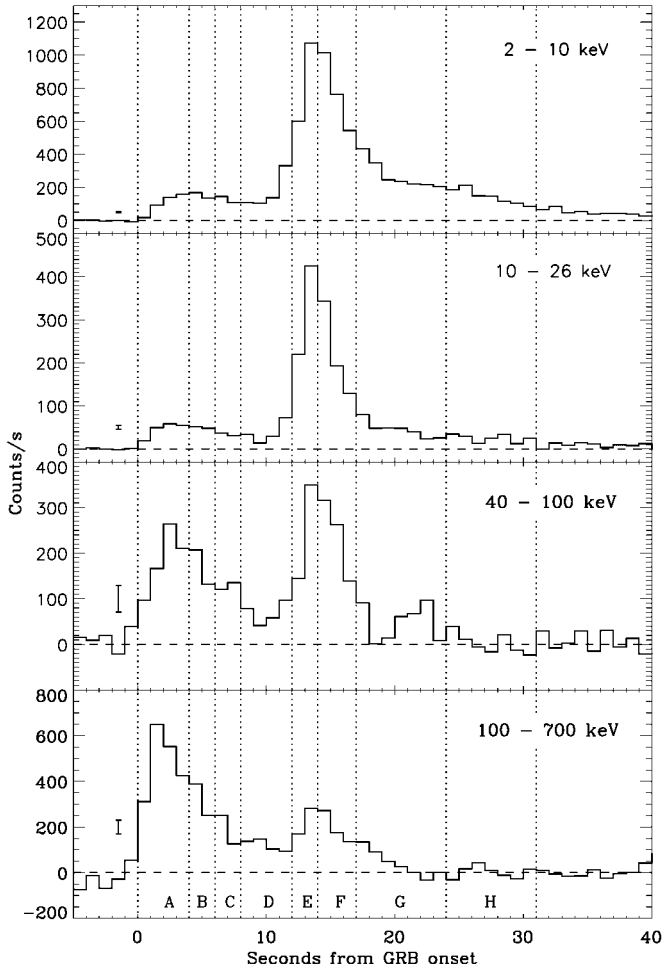

FIG. 1.—Light curves of GRB 990712 in four energy bands after background subtraction. The zero abscissa corresponds to 1999 July 12, 16:43:01.6 UT. The time intervals over which the spectral analysis was performed are indicated with vertical dotted lines.

of the energy of the first pulse with respect to the second: the peak flux of the first pulse increases with energy, while that of the second pulse decreases. The total duration of the event is about 20 s above 100 keV, but much longer (about 40 s) over the full 2–26 keV range. The spectral evolution of the event was studied by subdividing the GRB time profile into eight adjacent time intervals and performing an analysis of the spectrum of each interval (see Fig. 1). We fit the spectra with a power law [$N(E) \propto E^{\alpha}$], a broken power law, or a smoothed broken power law (Band et al. 1993) with photoelectric absorption (WABS model in XSPEC). We assumed the Galactic hydrogen column density N_H ($=4.52 \times 10^{20}$ cm^{-2}; Dickey & Lockman 1990) along the line of sight to the GRB. For the first three time slices, the fit was also performed leaving N_H free to vary, but unfortunately N_H was not constrained by the data. The fit results with a power law and a smoothed broken power law are given in Table 1. The results obtained with the broken power-law model were similar to those obtained with the smoothed broken power-law model and are not reported in Table 1. The spectra of the time intervals A and B, which correspond to the rise of the first pulse of the GRB, and the spectrum of interval D, which corresponds to the late tail of this pulse, are well fitted with a power-law model. The smoothed broken power-law model provides a good description of the spectra in time intervals E and F, which correspond to the core of the second pulse, while the power-law model again well describes the tail of the second pulse (intervals G and H). However, neither of these models provides a good description of the C spectrum ($\chi^2/\nu = 16/6$ for a power law and 16/5 for a smoothed broken power law). An excess with a significance level of about 3 σ is evident around 4 keV. We investigated a possible instrumental origin of this anomaly with negative results. The WFC high voltage, which is monitored every second, does not show any glitch in interval C. Given the accuracy of the readout (which dominates over statistical noise), this excludes gain changes higher than 0.01%. As in other GRB detections, the WFC ratemeters all show the GRB, even the ones that measure the illegal events, so we do not find any anomaly

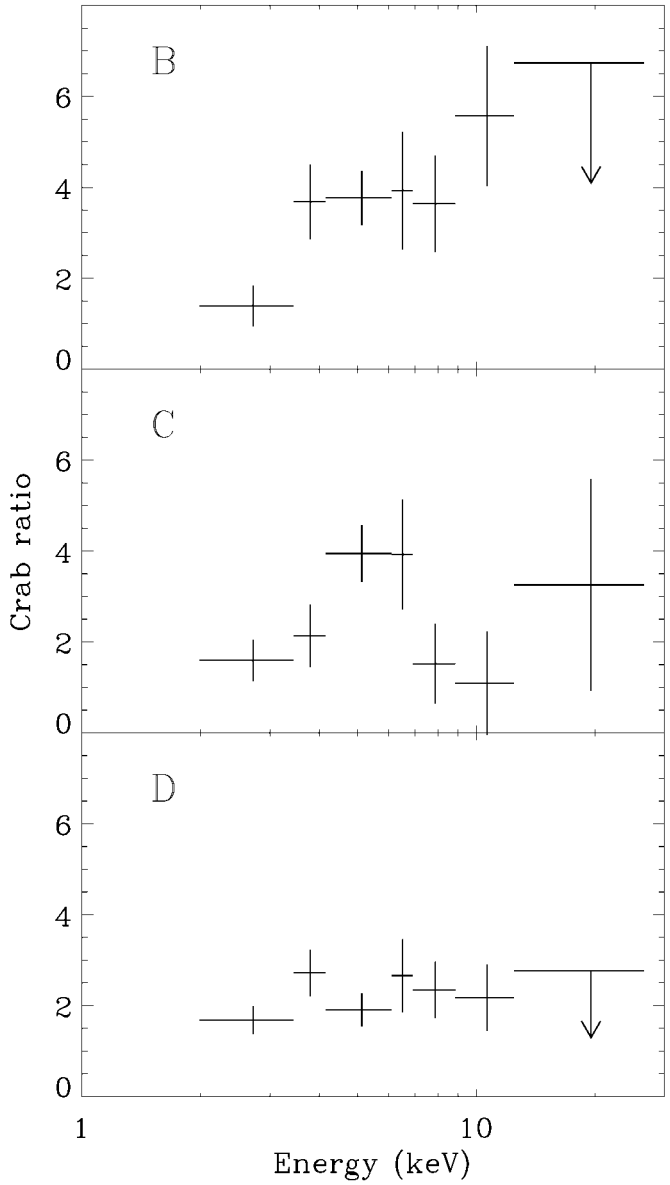

FIG. 2.—Ratio with the Crab count spectrum of the GRB 990712 spectra in time intervals B, C, and D, respectively, measured with the WFC2. The Crab spectrum used was measured when this source was observed at an angular offset similar to that of GRB 990712.

in this event. There are no dips or spikes of any sort, with a typical 3 σ upper limit of 10% per second of measurement (for a count rate of 700 counts s^{-1}). There is one thermometer that shows a small change about 10 s before the burst, but all other measurements do not show anything out of the ordinary. The count excess in the GRB spectrum of interval C is also clearly visible (see Fig. 2) in the ratio between the C count spectrum and the Crab spectrum measured when this source was observed at an angular offset similar to that of GRB 990712. For comparison, Figure 2 also shows the ratio with Crab of the spectra measured in intervals B and D, which precede and follow C, respectively. As can be seen, in interval B the greater hardness of the GRB spectrum (photon index of ~1.4; see Table 1) than that of the Crab is apparent, while in interval D the flatness of the Crab ratio is consistent with the similar slope of the GRB spectrum (see Table 1) with that of the Crab. A slight hint of the 4 keV excess in the spectrum also appears in interval B, but it is not statistically significant. We point out that the Crab ratio technique is adopted to discover cyclotron lines in the spectra of X-ray pulsars (e.g., Dal Fiume et al. 2000).

The addition of a Gaussian function or a blackbody spectrum to a power-law model provides a good fit ($\chi^2/\nu = 1.6/5$ and $\chi^2/\nu = 6.2/6$, respectively) to the C spectrum. The best-fit parameters of both models are reported in Table 2. For a better determination of the Gaussian and blackbody parameters, the photon index α of the power-law model was kept fixed in the fit to the best-fit value, which is given by 1.34 ± 0.17 or 1.24 ± 0.20, depending on the model assumed for the feature, a Gaussian or a blackbody model, respectively. The count rate spectrum of interval C along with the best-fit curve of the power law plus blackbody model is shown in the top panel of Figure 3, while the ratio between the count spectrum and the best-fit power law alone is shown in the bottom panel. The excess counts to the power-law model are apparent. The evolution of the logarithmic power per photon decade [the $EF(E)$ spectrum] with the time from the GRB onset is shown in Figure 4. The emission feature during interval C is also apparent in this plot. The peak energy of the $EF(E)$ spectrum (see Table 1) is above our energy passband for the entire duration of the first pulse before suddenly becoming much lower (~10 keV) from the beginning of the second pulse.

From the spectral fits we derived GRB fluence and peak flux. The γ-ray (40–700 keV) fluence of the burst is $S_\gamma = (6.5 \pm 0.3) \times 10^{-6}$ ergs cm^{-2}, while the corresponding value found in the 2–10 keV band is $S_X = (2.60 \pm 0.06) \times 10^{-6}$ ergs cm^{-2}, with a ratio $S_X/S_\gamma = 0.40 \pm 0.03$, which is one of the highest values found with *BeppoSAX* (Frontera et al. 2000). The 2–700 keV fluence is given by $S_\gamma = (1.10 \pm 0.03) \times 10^{-5}$ ergs cm^{-2}. The γ-ray peak flux is $P_\gamma = 4.1 \pm 0.3$ photons cm^{-2} s, corresponding to $(1.3 \pm 0.1) \times 10^{-6}$ ergs cm^{-2} s^{-1}, while the

TABLE 2
BEST-FIT PARAMETERS OF THE TIME INTERVAL C SPECTRUM

Parameter	Power Law + Gaussian	Power Law + Blackbody
α	[1.34]	[1.24]
F_{PL}(1 keV) (cm^{-2} s^{-1})	1.95 ± 0.24	1.13 ± 0.14
E_{line} (keV)	4.4 ± 0.8	…
σ_{line} (keV)	1.4 ± 0.7	…
I_{line} ($\times 10^{-8}$ ergs cm^{-2} s^{-1})	2.7 ± 1.1	…
L_{line} ($\times 10^{57}$ photons s^{-1})	2.5 ± 0.9	…
kT_{bb} (keV)	…	1.3 ± 0.3
L_{bb} ($\times 10^{49}$ ergs s^{-1})	…	2.5 ± 0.6
χ^2/ν	1.6/5	6.2/6

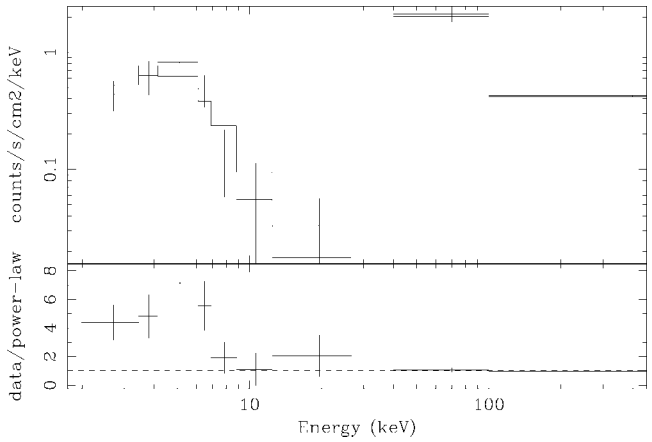

FIG. 3.—WFC + GRBM spectrum of GRB 990712 in time interval C, along with the best-fit curve obtained assuming a power law plus a blackbody model. *Bottom panel*: Ratio between the data and the best-fit power-law model alone.

corresponding 2–10 keV peak flux is $P_X = 41 \pm 4$ photons cm^{-2} s, corresponding to $(3.3 \pm 0.3) \times 10^{-7}$ ergs cm^{-2} s^{-1}.

4. DISCUSSION

From the redshift value of the optical afterglow of GRB 990712 ($z = 0.4331$; Vreeswijk et al. 2001) we can derive the X- plus γ-ray energy released in the main event. Assuming isotropic emission and a standard Friedman cosmology ($H_0 = 70$ km s^{-1} Mpc^{-1} and $q_0 = 0.5$), we get a 2–700 keV released energy of $E_{\rm rel} = (5.9 \pm 0.2) \times 10^{51}$ ergs. A sizeable fraction of this energy (~20%) is released between 2 and 10 keV. If we exclude the controversial case of GRB 980425/SN 1998bw (Galama et al. 1998; Kulkarni et al. 1998; Pian et al. 2000), GRB 990712, in addition to showing the lowest redshift, is one of the least energetic events.

GRB 990712 is marked by a peculiarity, which is noted here for the first time: the evidence of a broad emission feature at 4.4 keV, visible for 2 s, superposed on a power-law continuum model. It can be described by either a Gaussian profile with an FWHM of ~3 keV or a blackbody emission with $kT_{\rm bb} = 1.3$ keV. If we assume the Gaussian description, its centroid energy corrected for redshift ($E_0 = 6.4 \pm 1.1$ keV) is consistent with the energy of both an iron K fluorescence line and an iron recombination line. The interpretation of the emission feature as an iron recombination line is tempting, yet it makes some stringent demands on models; in fact, it requires much mass to be present within a few light-seconds of the burst site and requires this mass to be moving at Newtonian speeds. Vietri et al. (2001) derive the expected rate of photons for a narrow line:

$$\dot{N}_{\rm Fe} \approx \frac{4 \times 10^{52}}{T_7^{3/4}} \ {\rm s}^{-1} \left(\frac{M_{\rm Fe}}{1\ M_\odot}\right)\left(\frac{6 \times 10^{15}\ {\rm cm}}{R}\right), \qquad (1)$$

where T_7 and R are the electron temperature (in units of 10^7 K) and the external radius of the line-emitting medium, respectively, and $M_{\rm Fe}$ is the iron mass present in this medium. For a broad line, such as that in GRB 990712, the above value is an understimate by a factor of a few at most. Assuming $T_7 = 1, R = 6 \times 10^{15}$ cm, and $M_{\rm Fe} = 1\ M_\odot$, comparison with Table 2 shows that equation (1) underestimates the observed line luminosity by 4–5 orders of magnitude; inserting $R =$ 10 light-seconds in the above equation yields the correct line luminosity, but for a total mass of iron of *at least* $M_{\rm Fe} = 0.1\ M_\odot$. Assuming a realistic iron relative abundance (at least 1% of the total mass, if what we are seeing is a type I supernova, but more for any other hypothesis) shows that we must explain the presence of at least $10\ M_\odot$ of matter, at radii of a few light-seconds, with none of this obstructing the line of sight.

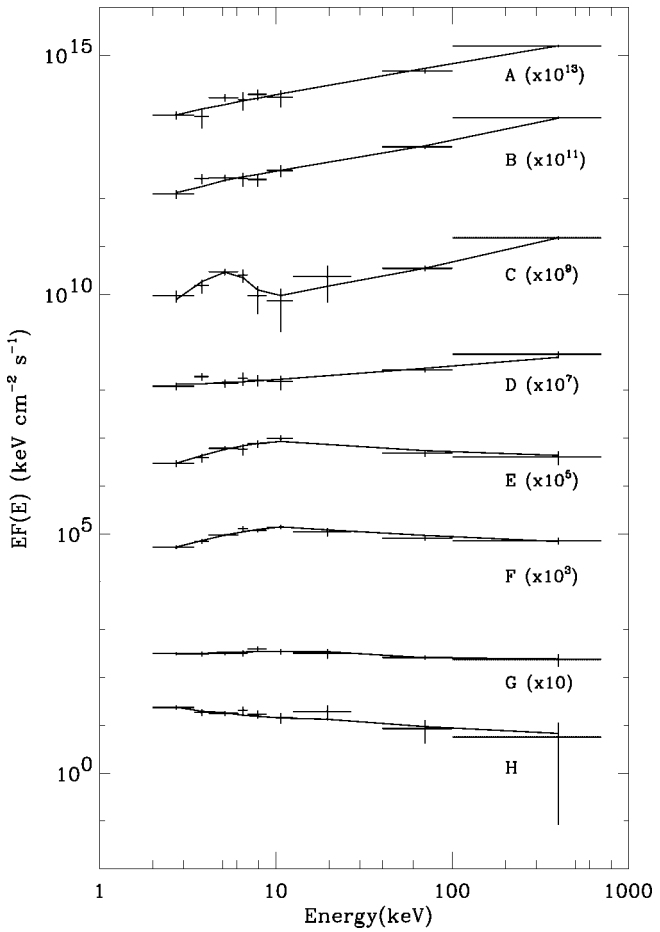

FIG. 4.—*EF*(*E*) spectrum of GRB 990712 in the time intervals in which we divided the burst time profile (see also Table 1). The GRB peculiar spectrum in interval C is apparent.

A more attractive possibility is that the observed feature is indeed thermal. Although we cannot definitely establish the thermal nature of the emission during interval C, we wish to remark that the fireball model can account naturally for the presence of these features. In fact, as remarked by both Paczyński (1986) and Goodman (1986), hyperrelativistic expansion naturally leads to the liberation of a fully thermal spectrum, at the time when the fireball expansion becomes optically thin. The initial absence, and later disappearance, of the peak in question does not create difficulties within the fireball model; it can easily be ascribed to inhomogeneities in the time structure of the relativistic wind, inhomogeneities that are in any case required in order to account for the burst subsecond variability. The fact that the peak, furthermore, appears during the tail of the first pulse of course makes the detection of the weaker thermal component easier (see the very revealing Fig. 2 of Mészáros & Rees 2000). If this spectral feature is indeed thermal in origin, within the fireball model there is a quantitative and independent check on this identification. In fact, the expected photospheric radius within the fireball model is (Mészáros & Rees 2000) $r_{\rm ph} = 1.2 \times 10^{13}$ cm$(L_{52} Y \eta_2^{-3})$, where L_{52} is the wind luminosity in units of 10^{52} ergs s^{-1}, $Y \approx$

1 is the number of electrons per baryon, and η_2 is the flow Lorentz factor η in units of 100. At this radius, the observed photospheric luminosity and temperature are $L_{\rm ph} = L_{52}(\eta/\eta_*)^{8/3}$ and $\Theta_{\rm ph} = \Theta_0\,(\eta/\eta_*)^{8/3}$, respectively, where $\eta_* \approx 10^3(L_{52}\mu_1^{-1}Y\Gamma_0)^{1/4}$ and $\Theta_0 = 1236\,(L_{52}^{1/2}\mu_1^{-1}\Gamma_0^{-1})^{1/2}$ keV, Γ_0 ($\geq$1) being the initial bulk Lorentz factor of the wind and μ_1 the mass, in units of 10 $M_\odot$, of the rotating black hole from 6 times the gravitational radius of which the fireball is assumed to start its expansion. By fitting simultaneously the observed temperature corrected for the redshift (1.86 keV) and the luminosity of the photosphere ($\sim 2 \times 10^{50}$ ergs s^{-1}), we find $\eta \approx 100Y^{1/4}\,(\mu_1^{-1}\Gamma_0^{11})^{1/54}$ and $L_{52} = 2(\mu_1\Gamma_0^{11})^{2/9}$. We thus see that the two independently determined observational parameters, blackbody temperature and luminosity, are well fitted by values of the theoretical parameters, η and L_{52}, well within the expected range. Assuming unit values for Y, Γ_0, and μ_1, L_{52} is about 100 times higher than the estimated 2–700 keV luminosity ($\sim 2 \times 10^{50}$ ergs s^{-1}) assuming isotropy. That would imply an efficiency of only 1% in the production of electromagnetic radiation.

In addition to the transient feature, the event shows a spectral evolution that is not typical of other GRBs observed with *BeppoSAX* (Frontera et al. 2000): the peak energy E_p of the $EF(E)$ spectrum (see Table 1 and Fig. 3) is constantly above our energy passband for the entire duration of the first pulse, while it takes a low value ($\sim$10 keV) with the onset of the second pulse.

This discontinuity can be the result of two successive electron acceleration episodes, giving rise to the first and the second pulses. The different peak flux behavior of the two pulses with energy, discussed in § 3, confirms this scenario. The emission feature is found only during the first acceleration event.

We thank John Stephen for his careful reading of the manuscript. Also, many thanks to the anonymous referee who helped us to improve this Letter.

REFERENCES

Amati, L., et al. 2000, Science, 290, 953
Antonelli, L. A., et al. 2000, ApJ, 545, L39
Arnaud, K. A. 1996, in ASP Conf. Ser. 101, Astronomical Data Analysis Software and Systems V, ed. G. H. Jacoby & J. Barnes (San Francisco: ASP), 17
Bakos, G., Sahu, K., Menzies, J., Vreeswijk, P., & Frontera, F. 1999, IAU Circ. 7225
Band, D., et al. 1993, ApJ, 413, 281
Böttcher, M., Dermer, C. D., Crider, A. W., & Liang, E. P. 1999, A&A, 343, 111
Dal Fiume, D., et al. 2000, Adv. Space Res., 25, 399
Dickey, J. M., & Lockman, F. J. 1990, ARA&A, 28, 215
Frontera, F., et al. 1997, A&AS, 122, 357
———. 1999, GCN Circ. 385 (http://gcn.gsfc.nasa.gov/gcn/gcn3/385.gcn3)
———. 2000, ApJS, 127, 59
Galama, T., et al. 1998, Nature, 395, 670
Ghisellini, G., et al. 2000, MNRAS, 316, L45
Goodman, J. 1986, ApJ, 308, L47
Heise, J., et al. 1999, IAU Circ. 7221
Jager, R., et al. 1997, A&AS, 125, 557
Kulkarni, S. R., et al. 1998, Nature, 395, 663
Mészáros, P., & Rees, M. J. 1998, ApJ, 502, L105
———. 2000, ApJ, 530, 292
Paczyński, B. 1986, ApJ, 308, L43
Pian, E., et al. 2000, ApJ, 536, 778
Piro, L., et al. 1999, ApJ, 514, L73
———. 2000, Science, 290, 955
Tavani, M. 1996, ApJ, 466, 768
Vietri, M., Ghisellini, G., Lazzati, D., Fiore, F., & Stella, L. 2001, ApJ, in press
Vreeswijk, P. M., et al. 2001, ApJ, 546, 672
Yoshida, A., et al. 1999, A&AS, 138, 433